

Removal of Lead (II) from Water by Agro-Industrial by-Products Adsorbent

Fatma TOMUL^{*1}, Yasin ARSLAN², Azime Büşra YAVUZ¹

¹Mehmet Akif Ersoy University, Faculty of Arts and Science, Chemistry Department, 15100, Burdur

²Mehmet Akif Ersoy University, Faculty of Arts and Science, Nanoscience and Nanotechnology Department, 15100, Burdur

(Alınış / Received: 31.05.2018, Kabul / Accepted: 15.08.2018, Online Yayınlanma / Published Online: 18.09.2018)

Keywords

Lead,
Adsorption,
Walnut shell,
Lemon peel,
Activation

Abstract: Pb(II) adsorption from the water using adsorbents such as acid and/or base activated walnut shell and lemon peel was carried out in a continuous stirring batch system. The original and activated adsorbents were characterized by SEM-EDS and FTIR analyses. SEM photographs of both adsorbents showed that while the presence of irregularly shaped and layered structures were observed before activation, more porous and curved surfaces were observed after activation. Adsorption studies showed that the activation was effective for increasing the adsorption efficiency and while more than 50% of the lead ions were removed at the first 10 min, the equilibrium was reached at 180 min. Furthermore, they showed that the adsorption rate was determined by a pseudo second order kinetic model. Additionally, Freundlich and Langmuir isotherm models were investigated for Pb(II) adsorption on WS-NaOH and LP-HNO₃ adsorbents and it was found that the equilibrium data were more suitable for Freundlich model.

Agro-Endüstriyel Yan Ürün Adsorbentler ile Sulardan Kurşun (II) Giderilmesi

Anahtar Kelimeler

Kurşun,
Adsorpsiyon,
Ceviz kabuğu,
Limon kabuğu,
Aktivasyon

Özet: Bu çalışmada, Pb(II) iyonlarının, asit ve/veya baz ile aktive edilmiş ceviz ve limon kabuğu gibi adsorbentler ile adsorpsiyonu kesikli çalışan bir adsorpsiyon sisteminde gerçekleştirilmiştir. Orijinal ve aktive edilmiş adsorbentler SEM-EDS ve FTIR analizleri ile karakterize edilmiştir. Her iki adsorbentin SEM fotoğraflarında, aktivasyondan önce düzensiz şekilli ve tabakalı yapıların varlığı gözlenirken, aktivasyondan sonra daha gözenekli ve kıvrımlı yüzeylerin oluştuğu görülmüştür. Adsorpsiyon çalışmaları, aktivasyonun adsorpsiyon veriminin artışında etkili olduğunu ve kurşun iyonlarının % 50'sinden daha büyük bir kısmının ilk 10 dakika içerisinde giderildiğini, 180 dakikada ise dengeye ulaşıldığını göstermiştir. Ayrıca, adsorpsiyon çalışmaları adsorpsiyon hızının yalancı ikinci dereceden kinetik modeli ile tanımlanabileceğini de göstermiştir. Freundlich ve Langmuir izoterm modelleri de WS-NaOH ve LP-HNO₃ adsorbentleri üzerindeki Pb (II) iyonlarının adsorpsiyonunu tanımlamak için uygulanmış ve denge verilerinin Freundlich modeline daha uygun olduğu bulunmuştur.

1. Introduction

Water is an indispensable renewable resource to sustain life on Earth [1]. Contamination of natural waters with heavy metals is a global problem. Industrial activity, wastewater and domestic wastewater is the main source of pollution in the water. Natural resources such as rainwater and erosion also cause heavy metal pollution. The biggest problem with heavy metals is that they can stay in the environment for a long time without deterioration and have the potential to accumulate in different parts of the body. For this reason, the detection of heavy metals in the water is a worldwide field of

work requiring attention and prevention [2]. Na, K, Ca, Mg, Bi, Sb, Fe and Al are the main metals passing into the water from the soil. On the hand, metals such as Al, Pb, Cd, Ni, Cu, Hg, As, Cr, Co, Mn and Zn are mixed into the water through industry and domestic wastes. Hg, Cd, Bi, Sb, Pb and As are the most dangerous metals that can be found in water. Lead is one of the most important heavy metals [3]. It is diffused into the atmosphere in metallic form and/or its compounds and causes environmental pollution [4, 5] by some industrial applications such as mining process, battery production, lead alkaline production, welding/soldering works, painting, printing, ceramic and plastic industries, water pipes and wire cables [6,

7]. Lead concentration can be observed up to 500 µg in soft water. The maximum lead level that can be found in drinking water is specified by World Health Organization (WHO) as 10µg/L [8].

When lead concentration in water samples was above the permissible value, it caused some detrimental effects such as anemia, nephritic syndrome, digestion and nervous system destruction [9-11]. Therefore, removal of lead and/or its compounds from water samples was an important environmental problem. For this reason, economic and environmentally friendly treatment methods should be developed. Among them, adsorption was generally preferred method since its application was easy and successful to remove toxic ions from sample [12]. In last decades, agro-agricultural by-products obtained from wastes were used as alternative to active carbon due to some advantages, such as low cost, easy to application and higher treatment capacity for metal adsorption [13, 14]. Additionally, acid and/or base treatment was also widely used for chemical activation of agricultural wastes [15].

In this study, lead (II) removal from the water samples was carried out in a continuous stirring batch system using agro-industrial by-products adsorbents, such as walnut shell (WS) and lemon peel (LP) which were activated with both HNO₃ and NaOH, respectively. Additionally, the effects of adsorbent amount, pH, temperature and contact time on the adsorption rate of lead (II) were also investigated to find optimum experimental conditions for removal of lead (II).

2. Material and Method

In this study, WS and LP modified with both HNO₃ and NaOH were used as the adsorbents. All chemicals used for the preparation of adsorbents are of analytical purity. Deionized water purification system (PURIS, 18 MΩ.cm) was used in the preparation of the all solutions.

2.1. Preparation of adsorbents

WS and LP were obtained from the local market in Burdur, Turkey. At first, WS and LP were washed with tap water and deionized water to remove contaminants, respectively. Then, they were dried at 348 K for 55 h and milled and agitated for 24 h using 1.0 mol L⁻¹ sodium hydroxide (Merck) and 0.1 mol L⁻¹ nitric acid (Merck) in the ratio of 1/10 (m/v), respectively. Afterwards, they were washed again with deionized water to remove acid and/or base in the reaction medium and then dried again at 348 K for 24 h before use. The prepared adsorbents were stored until experiment. The adsorbents modified with both acid and base were coded as WS-NaOH and LP-HNO₃. In addition, lead adsorbed by WS-NaOH and LP-HNO₃ were coded as WS-NaOH-Pb and LP-HNO₃-Pb.

2.2. Adsorption

Pb(II) adsorption was investigated at 500 rpm stirring speed in a continuous stirring batch system. The calibration solutions were prepared by diluting of a 1000 mg L⁻¹ stock solution prepared from Pb(NO₃)₂. Effect of some experimental parameters, such as adsorbent amount (between 0.5 and 10 g L⁻¹), pH (between 4 and 8) and temperature (at 298, 308 and 318 K) were investigated using 20 mg L⁻¹ Pb(II) adsorbate solution. However, apart from the effect of the adsorbent amount, pH and temperature on adsorption, they were chosen as 10 g L⁻¹, 6 and 298 K, respectively. Additionally, the effect of the contact time was investigated using different Pb(II) concentrations between 20 and 100 mg L⁻¹ and 10 g L⁻¹ adsorbent amount based on time period of 10-240 min. Furthermore, adsorption studies were repeated to determine the reusability of the adsorbents. After each adsorption step, the samples were filtered and re-used after drying at 333 K for 24 h.

The amount of Pb(II) remaining in the solution was determined using a single beam atomic absorption spectrometer (ATI Unicam 939 model) with deuterium background correction system. The adsorption efficiency (%) and capacity (q_e, mg g⁻¹) were calculated using the following equations:

$$Adsorption(\%) = \frac{(C_0 - C_e)}{C_0} * 100 \quad (1)$$

$$q_e = \frac{(C_0 - C_e) * V}{m} \quad (2)$$

C₀ (mg L⁻¹) and C_e (mg L⁻¹) showed Pb(II) concentrations before and after adsorption, respectively. Furthermore, V (L) and m (g) showed the solution volume and adsorbent amount, respectively.

2.3. Characterization of adsorbents

The surface morphology and composition of the original WS and LP, activated and lead adsorbed activated WS and LP adsorbents were analysed using SEM (Phillips XL-30 S FEG) with EDX detector, respectively and surface photographs and elemental composition graphs were obtained. FTIR (Perkin Elmer BX) spectra with KBr (1 mg sample/100 mg KBr) were used to identify functional groups of all samples.

3. Results

3.1. Adsorption studies

3.1.1. Adsorbent type and amount

The adsorbent amount was an important factor to determine the adsorption efficiency for any

contaminant concentration. The adsorbents (WS, WS-HNO₃, WS-NaOH, LP, LP-HNO₃, and LP-NaOH) amounts were investigated between 0.5 and 10 g L⁻¹. When the the adsorbent amount was increased, the lead removal was also increased and the highest adsorption efficiency for the adsorbent amounts was reached at a concentration of 10 g L⁻¹ adsorbent shown in Figure 1 (a1 and a2). Adsorption efficiency was increased with increasing the amount of adsorbent owing to the increasing active surfaces of adsorbents which were also suitable for adsorption [16, 17]. Although the adsorption efficiency was increased after the modification with HNO₃ and NaOH in both adsorbents, the activation with NaOH for WS and HNO₃ for LP was found to be more effective based on the adsorption efficiency. The adsorption efficiency of original WS (81%) for 10 g L⁻¹ adsorbent amount was increased to 87% and 99% for WS-HNO₃ and WS-NaOH adsorbents, respectively. On the other hand, the adsorption efficiency of original LP (79%) for 10 g L⁻¹ adsorbent amount was increased to 99% and 92% for LP-HNO₃ and LP-NaOH adsorbents respectively. Therefore, 10 g L⁻¹ adsorbent amount for WS-NaOH and LP-HNO₃ adsorbents were selected. The literature studies showed that the adsorption efficiencies/adsorption capacities of fruit/vegetable wastes were increased by acid and/or base activation and the acid-activated fruit peels had higher adsorption capacity than that of the base-activated shells [18, 19]. On the other hand, there are studies in the literature that show that the adsorption capacity of fruit shells increases more with base activation [20, 21]. Acid and/or base activation caused to the formation of new adsorption sites on the adsorbent surface leading to an increase in adsorption efficiency.

3.1.2. pH

The different pH values (between 4 and 8) were investigated using 20 mg L⁻¹ Pb(II) adsorbate solution at 298 K. Both adsorbents produced high adsorption rates at pH 4 and 6 at 10 min and reached a maximum at 240 min. However, by increasing the pH from 6 to 8, the efficiency of adsorption was considerably reduced shown in in Figure 1 (b1 and b2) since the probability of adhesion to the surface of the adsorbents was reduced owing to strong acidic environments including more H⁺ concentration. Additionally, at higher pH values, the positive charge density on the surface were decreased while the negative charge density (due to OH⁻ ions) was increased, resulting in an increase in adsorption. However, it was also possible that Pb(II) could be precipitated as hydroxide in basic solution. This caused to a decrease in adsorption efficiency [22]. The similar results were reported with single-walled carbon nanotubes-doped WS composite [23], raw and acid-activated Citrus limetioides peel and seeds [24], and tripolyphosphate-modified waste Lyocell fibers

[25] for Pb(II) adsorption. Furthermore, when the literature was examined, pH 6 was used for the adsorption of Pb(II) in the presence of different agro-industrial by product adsorbents [26-29].

3.1.3. Temperature

Temperature was changed between 298 and 318 K and results were shown in Figure 1 (c1 and c2), respectively. The adsorption efficiency was decreased by increasing temperature due to the exothermic process for lead adsorption on the adsorbents.

To verify the feasibility of the adsorption, several thermodynamic functions (ΔG , ΔH and ΔS) were determined using the following equations [30-33].

$$\ln K_d = \frac{\Delta S}{R} - \frac{\Delta H}{RT} \quad (3)$$

$$\Delta G = \Delta H - T\Delta S \quad (4)$$

where R was 8.314 J mol⁻¹ K⁻¹, T (K) was temperature and K_d was the distribution coefficient of the adsorbate (dimensionless), $(\frac{q_e}{C_e})$. q_e was the

equilibrium Pb(II) concentration on the adsorbent (mg L⁻¹) and C_e was the equilibrium Pb(II) concentration in the solution (mg L⁻¹). ΔH and ΔS were found from the slope and intercept of a graph between $\ln K_d$ and $\frac{1}{T}$ (not shown). Thermodynamic

parameters were given in Table 1. The enthalpy changes for adsorption onto WS-NaOH and LP-HNO₃ were found to be -44.50 and -42.92 kJ mol⁻¹, respectively. Negative ΔH values indicated that Pb(II) adsorption was an exothermic process. The ΔS for adsorption onto WS-NaOH and LP-HNO₃ were found to be -0.125 and -0.118 kJ mol⁻¹K⁻¹, respectively. Negative ΔS values revealed that the disorder of the solid/solution interface was decreased during Pb(II) adsorption [34]. Sudha et al. reported negative ΔH and ΔS value for the adsorption of Pb(II) onto the raw and acid-activated Citrus limetioides peel and seeds [24].

ΔG values for Pb(II) adsorption were found to be -7.31, -5.67, -4.82 kJ mol⁻¹ for WS-NaOH and -7.76, -5.69, -5.42 kJ mol⁻¹ for LP-HNO₃ at 298, 308, 318 K, respectively (Table 1). As seen, the ΔG values for adsorption onto WS-NaOH and LP-HNO₃ were negative at wide temperature range. These results indicated that the adsorption of Pb(II) onto WS-NaOH and LP-HNO₃ were spontaneously occurred and this process was thermodynamically feasible. According to results, (negative ΔH and ΔS values), Pb(II) adsorption should be carried out at low temperatures.

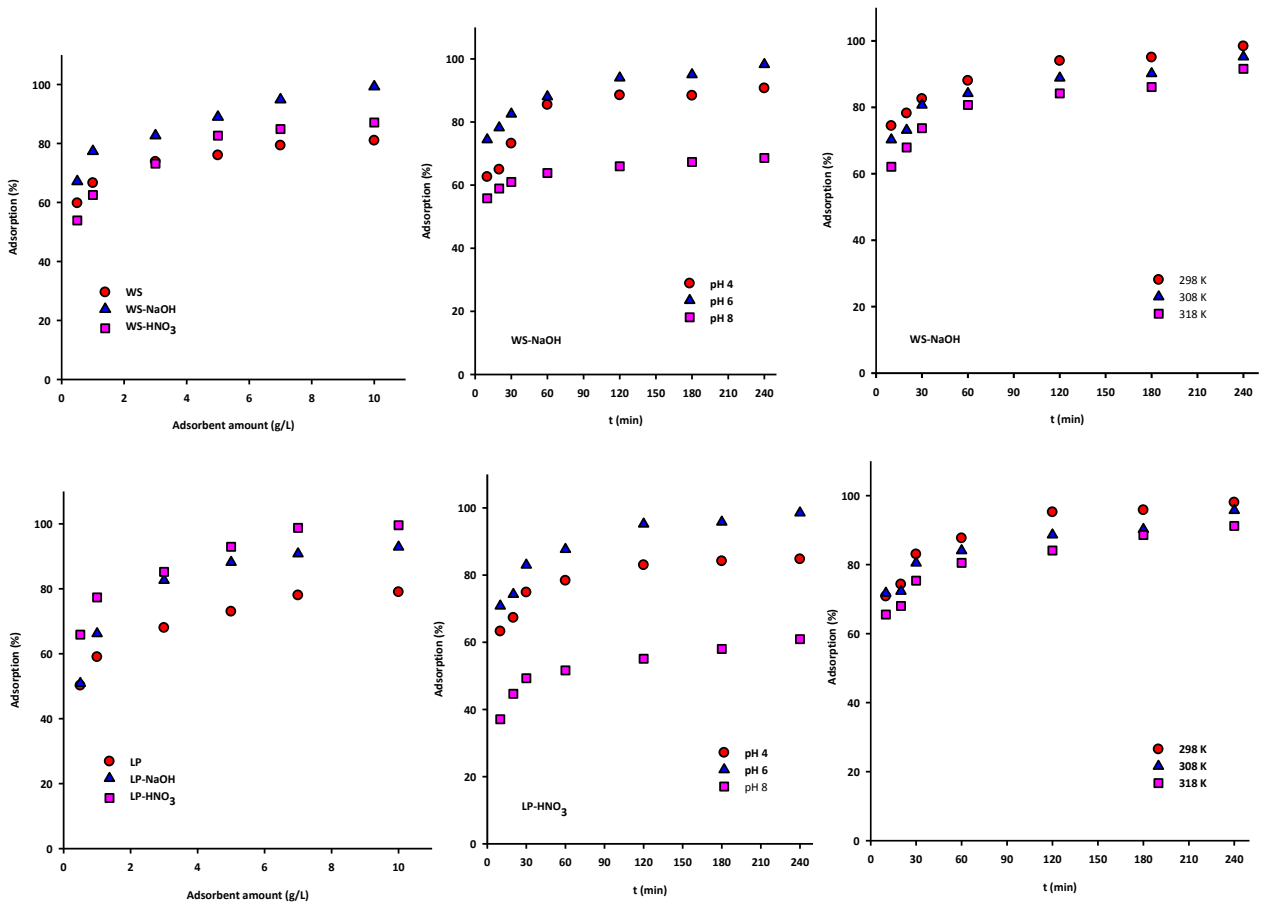


Figure 1. Pb(II) adsorption based on adsorbent amount (a1 and a2), pH (b1 and b2) and temperature (c1 and c2).

Table 1. Distribution coefficients and thermodynamic parameters for the adsorption of Pb(II) on WS-NaOH and LP-HNO₃ samples at different temperatures [Pb(II) adsorbate solution: 20 mg L⁻¹, adsorbent amount: 10 g L⁻¹, pH 6]

T (K)	K _d	ΔG (kJ mol ⁻¹)	ΔH (kJ mol ⁻¹)	ΔS (kJ mol ⁻¹ K ⁻¹)
WS-NaOH				
298	19.09	-7.31	-44.50	-0.125
308	9.17	-5.67		
318	6.19	-4.82		
LP-HNO ₃				
298	22.89	-7.76	-42.92	-0.118
308	9.24	-5.69		
318	7.76	-5.42		

3.1.4. Adsorption kinetics and contact time

To determine the equilibrium time and adsorption kinetics, the effect of contact time was investigated based on different initial Pb(II) concentrations. The results were given in the Figure 2. More than 50% of the Pb(II) were removed at first 10 min and the equilibrium was reached at 180 min for all initial concentrations. It was seen that the increase in the efficiency of adsorption in the subsequent contact times after equilibrium times was not significant. Initially, the rapid adsorption of lead ions was due to multitude of sites available for adsorption at the adsorbent surface, while the adsorption was slowing as these sites which were gradually coated over time.

The lead removal efficiencies of both adsorbents

were close to each other by comparing the results in Figure 2. Adsorption efficiencies of WS-NaOH and LP-HNO₃ adsorbents were found to be 74.42% and 70.81% at 10 min for 20 mg L⁻¹ Pb (II), respectively. On the other hand, adsorption efficiency of WS-NaOH and LP-HNO₃ adsorbents was increased to 95.02% and 95.81% at 180 min for 20 mg L⁻¹ Pb (II), respectively. However, the increase in adsorption efficiency for Pb(II) was remained extremely low after 180 min. For this reason, kinetic data were calculated by considering 180 min contact time. As adsorbent surface was saturated with Pb(II) under equilibrium conditions, a longer contact time was not a practical. In addition, adsorption efficiencies were decreased for both adsorbents when initial concentration was increased. For example, when

initial concentration was increased from 20 mg L⁻¹ to 100 mg L⁻¹ at 240 min, adsorption yields for the WS-NaOH and LP-HNO₃ adsorbents were decreased from 98.40% to 82.53% and from 98.05% to 84.87% respectively. As the ratio of lead ion/adsorbent was increased, excess metal ions in the atmosphere were saturated on the sites. Thus, the propulsive power was increased and the adsorption was decreased. Since lead concentration was increased, adsorption efficiency was decreased but its capacity was increased. This result might be explained because all sites was suitable for adsorption at higher lead concentrations.

The kinetic models were also important for the adsorption rate. In this study, to determine the adsorption rate for Pb(II) for WS-NaOH and LP-HNO₃ adsorbents, pseudo-first-order and pseudo-second

order kinetic models were employed. They were expressed by following equations [35, 36].

$$\ln(q_e - q_t) = \ln q_e - k_1 t \tag{5}$$

$$\frac{t}{q_t} = \frac{1}{k_2 q_e^2} + \frac{t}{q_e} \tag{6}$$

First-order adsorption rate constants (k_1) were obtained using both slope and constant of the straight lines by plotting $\ln (q_e - q_t)$ versus time. On the other hand, second-order adsorption rate constants (k_2) and equilibrium concentrations (q_e) values were calculated using both slope and constant of the straight lines by plotting t/q_t versus time. The kinetic models of them obtained at 298 K were given in Figure 3 and the kinetic parameters of them were shown in Table 2.

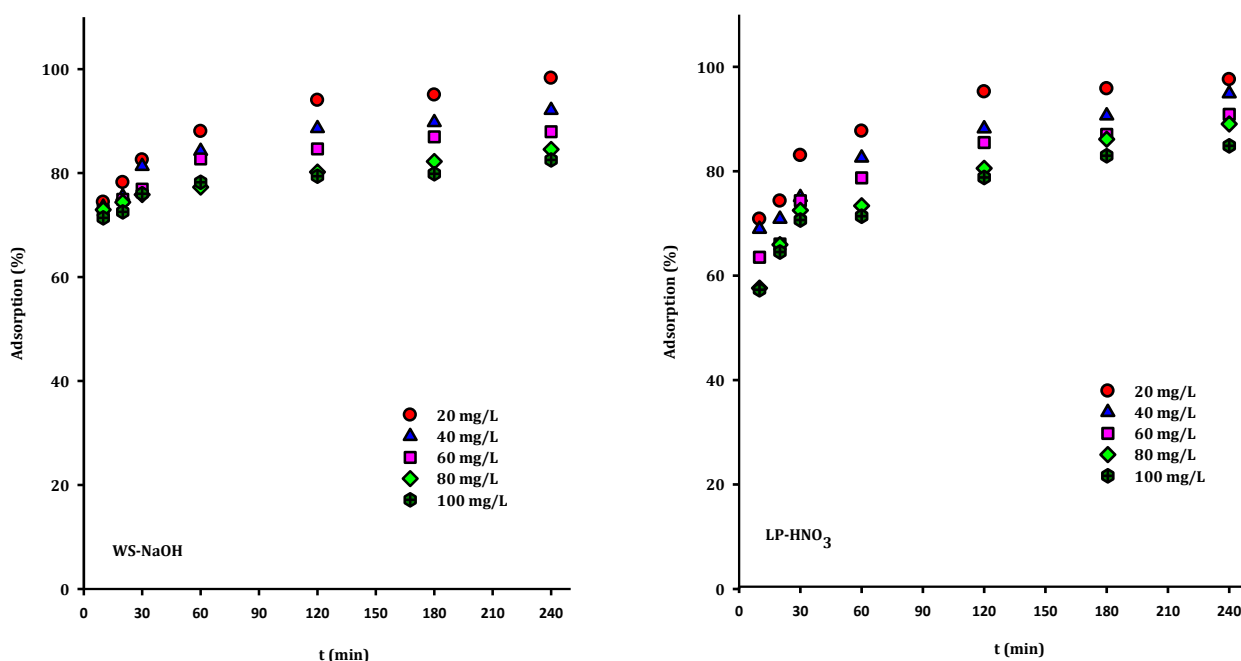


Figure 2. Effect of contact time on the adsorption of Pb(II) [10 g L⁻¹ adsorbent amount, pH 6 and T=298 K

Table 2. Kinetic parameters for the adsorption of Pb(II) on WS-NaOH and LP-HNO₃ [10 g L⁻¹ adsorbent amount, pH 6 and T=298 K]

[Pb(II)] (mg L ⁻¹)	q _{e-exp.} (mg g ⁻¹)	Pseudo-first order			Pseudo-second order		
		q _e (mg g ⁻¹)	k ₁ (min ⁻¹)	R ²	q _e (mg g ⁻¹)	k ₂ (g mg ⁻¹ min ⁻¹)	R ²
WS-HaOH							
20	1.90	0.58	0.027	0.991	1.99	0.084	0.999
40	3.59	0.83	0.024	0.988	3.72	0.058	0.999
60	5.22	0.95	0.017	0.953	5.34	0.046	0.999
80	6.58	0.83	0.013	0.992	6.78	0.038	0.999
100	7.99	1.02	0.027	0.975	8.25	0.041	0.999
LP-HNO ₃							
20	1.92	0.82	0.034	0.973	2.00	0.079	0.999
40	3.63	1.12	0.020	0.998	3.85	0.033	0.999
60	5.22	1.88	0.025	0.987	5.55	0.023	0.999
80	6.89	2.13	0.013	0.921	7.28	0.014	0.998
100	8.30	2.52	0.015	0.939	8.68	0.014	0.999

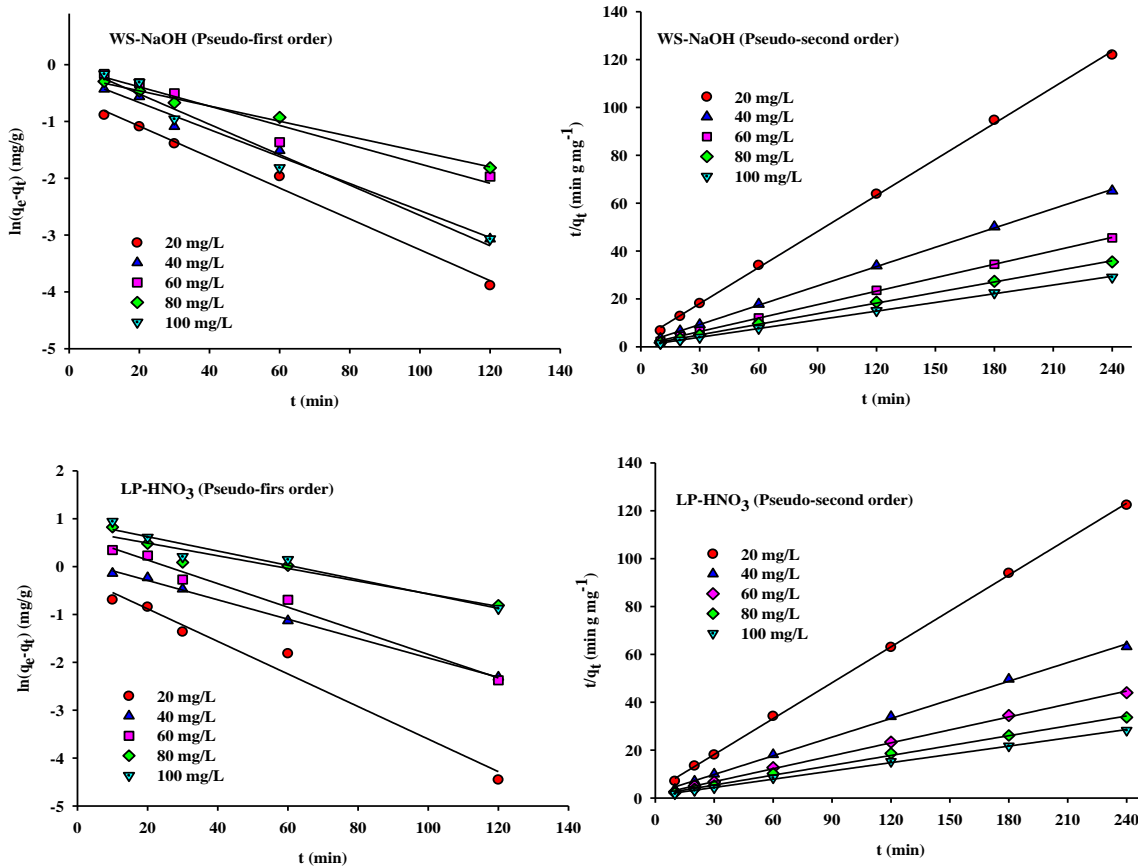


Figure 3. Pseudo-first order and pseudo-second order plots for the adsorption of different Pb(II) concentration at 298 K

The correlation coefficients were higher for the second order equation indicating that Pb(II) adsorption was belonging to second order kinetic model. Furthermore, the theoretical (q_e) obtained from the linear equations was near to the experimental ($q_{e, exp}$) values. This experimental data was suitable for the second order kinetic model. Therefore, Pb(II) adsorption for WS-NaOH and LP-HNO₃ adsorbents was suitable for second order kinetic model. When the second order rate constants (k_2) for WS-NaOH and LP-HNO₃ adsorbents were examined, the adsorption rate of WS was higher than that of LP.

3.1.5. Initial concentration and adsorption isotherms

Since initial concentration was an important parameter to determine the adsorption capacity of adsorbent, its effect for WS-NaOH and LP-HNO₃ adsorbents was also investigated. The adsorbed Pb(II) amount for both adsorbents was increased when Pb(II) concentration was increased. When Pb(II) initial concentration was increased from 20 mg L⁻¹ to 100 mg L⁻¹, adsorbed Pb(II) amount for WS-NaOH and LP-HNO₃ adsorbents was also increased from 1.97 mg g⁻¹ to 8.25 mg g⁻¹ and from 1.96 mg g⁻¹ to 8.49 mg g⁻¹, respectively. It showed that adsorption was dependent on initial concentration. On the other hand, when the results obtained from the viewpoint of adsorbents were examined, the adsorption

capacities were close to each other for both adsorbents.

Additionally, adsorption isotherms were used for determination of both adsorption capacities of the adsorbents and interaction between the adsorbent and the adsorbate. Two typical isotherm models, Langmuir and Freundlich isotherm equations, were used to analyse isotherm data of lead adsorption with modified WS and LP and linear equations were expressed as follows [37-39].

$$\frac{C_e}{q_e} = \frac{1}{q_m K_L} + \frac{C_e}{q_m} \tag{7}$$

In the Langmuir isotherm equation, q_m (mg g⁻¹) and K_L were the isotherm constants showing the maximum adsorption capacity and binding energy, respectively. When C_e values were plotted versus the $\frac{C_e}{q_e}$, the slope of linear line was $\frac{1}{q_m}$ and constant of

it was $\frac{1}{K_L q_m}$.

$$\ln q_e = \ln K_F + \frac{1}{n} \ln C_e \tag{8}$$

The K_F and n values in Freundlich isotherm equation showed the adsorption capacity and the heterogeneity of the adsorbent surface sites, respectively. The K_F and n values were calculated by plotting the $\ln q_e$ versus the $\ln C_e$ in the linear Freundlich equation. In this study, Pb(II) adsorption on WS-NaOH and LP-HNO₃ adsorbents was modelled using both Langmuir and Freundlich isotherms. Their isotherm constants and correlation coefficients were summarized in Table 3. When R^2 values were examined, the adsorption process corresponded to Freundlich isotherm equation. When the K_F values calculated from the Freundlich isotherm model were examined, acid-activated LP adsorbent had higher adsorption capacity than that of base-activated WS adsorbent. The K_F value was obtained as 2.76 for WS-NaOH and 2.85 for LP-HNO₃, respectively. The n value in the Freundlich model showed the deviation from the linearity. The Freundlich isotherm model was suitable due to the fact that n value was in the range between 1 and 10. This study confirmed the suitability of the Freundlich isotherm model in which n values obtained for both adsorbents were in the range between 1 and 10 (Table 3). The results for the Freundlich isotherm model showed that the adsorption was occurred on heterogeneous solid surface and SEM photographs also supported this result (Figure 4).

3.2. Reusability

Industrial applications were long-term reusability of adsorbents preserving their adsorption efficiency/adsorption capacity. Additionally, the high reusability of an adsorbent was an important for economically. To determine reusability of adsorbents, 4 cycles adsorption experiments for both adsorbents were performed. The adsorption was conducted in the experimental conditions of 20 mg L⁻¹ Pb(II) adsorbate solution, $T=298$ K, pH 6, $m_{\text{adsorbent}}=10$ g L⁻¹. After 4 cycles adsorption experiments, adsorption efficiencies of WS-NaOH-Pb and LP-HNO₃-Pb were found to be approximately 94% and 88%, respectively. These results showed that the adsorbents might be successfully used as four times.

Table 3. Langmuir and Freundlich model parameters

	$q_{m, \text{exp.}}$ (mg g ⁻¹)	Langmuir			Freundlich		
		q_m (mg g ⁻¹)	K_L (L mg ⁻¹)	R^2	K_F (mg g ⁻¹) (L mg ⁻¹) ^{1/n}	n	R^2
WS-NaOH	8.25	9.18	0.28	0.934	2.76	2.85	0.978
LP-HNO ₃	8.49	9.71	0.35	0.969	2.85	2.48	0.998

Table 4. Chemical composition (mass%) of original, activated WS and LP and lead adsorbed activated WS and LP

	WS	WS-NaOH	WS-NaOH-Pb	LP	LP-HNO ₃	LP-HNO ₃ -Pb
C	48.48	41.59	40.33	41.80	43.45	43.65
O	46.77	50.63	49.76	53.12	52.99	53.43
Ca	4.75	4.26	3.92	2.39	0.92	
Na		3.53	3.41	0.25	0.25	0.08
K				2.44	0.11	
N					2.28	
Pb			2.62			2.85

3.3. Characterization studies

3.3.1. SEM-EDX

The surface images of WS, WS-NaOH, WS-NaOH-Pb, LP, LP-HNO₃ and LP-HNO₃-Pb adsorbents were shown in Figure 4. While the presence of irregularly shaped and layered structures for both WS and LP adsorbents were observed before activation, porous and curved surfaces were observed after activation of WS and LP adsorbents with acid and/or base and lead adsorption. It showed that activation process was effective for pore formation. The elemental compositions (Table 4) showed that the original WS and LP contained mainly C and O, and smaller amounts of Ca, Na and K. The high C and O contents of these adsorbents were due to the presence of polysaccharides such as cellulose, hemicellulose, lignin and pectin [15, 40, 41]. Changes in the composition of the WS and LP adsorbents were observed depending on the activation and adsorption process. In addition, the presence of Na and Pb for the WS sample and N and Pb for the LP sample were observed with SEM-EDX analysis (Table 4).

3.3.2. FTIR

FTIR spectra of WS and WS-NaOH, LP and LP-HNO₃ were shown in Figure 5 and it was evaluated according to the literature [40-42]. The band at 3538-3340 cm⁻¹ for WS was due to hydroxyl groups or adsorbed water. The bands at 2924 cm⁻¹ were due to C-H stretching vibrations in methyl and methylene groups whereas the bands at 1443 and 1318 cm⁻¹ were due to C-H bending vibrations in methyl and methylene groups. Furthermore, while the bands at 1622 cm⁻¹ and 1521 cm⁻¹ were owing to C = C stretching and skeletal vibration, respectively, the band at 1055 cm⁻¹ were owing to C-O tension vibrations in alcohols, phenols or ether groups. On the other hand, the band at 1742 cm⁻¹ due to the C = O stretching vibrations was not observed after activation with sodium hydroxide and lead adsorption (Figure 5a) [40, 41].

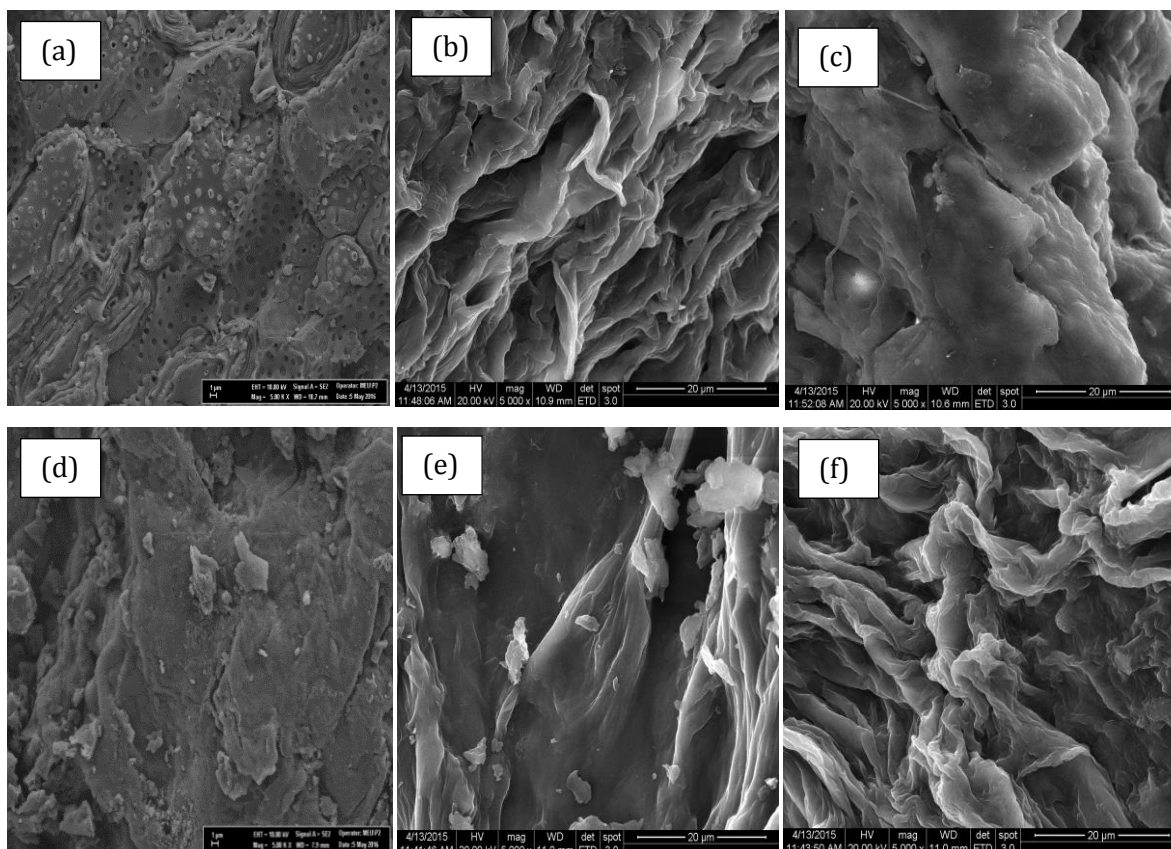


Figure 4. SEM micrographs of (a) WS-5000x (b) WS-NaOH-5000x (c) WS-NaOH-Pb-5000x (d) LP-5000x (e) LP-HNO₃-5000x and (f) LP-HNO₃-Pb-5000x

When the FTIR spectra of the original and nitric acid-activated LP adsorbents were examined (Figure 5b), there were no significant structural changes except for peak intensity. For the LP sample, the intensity of the characteristic cellulose peak observed at 1000-1200 cm⁻¹ in fingerprint region was decreased after the activation with nitric acid. Peaks at 1600 and 1800 cm⁻¹ indicated free and esterified carboxyl groups and they were used to identify pectins. The peak intensities in this region were also decreased after the activation. Especially the reduction of the

ester peak observed at 1743 cm⁻¹ after the activation might be explained because of decreasing the carboxyl groups linked to the cellulose and pectin chains. The broad peak at 3200 and 3600 cm⁻¹ indicated the presence of hydroxyl groups linked to molecules, such as cellulose and pectin [42]. Similar results were also obtained with base-activated LP by Singh and Shukla [43]. No change was observed in the FTIR spectra of both adsorbents after lead adsorption apart from peak intensity. This behaviour indicated that the adsorption was physical.

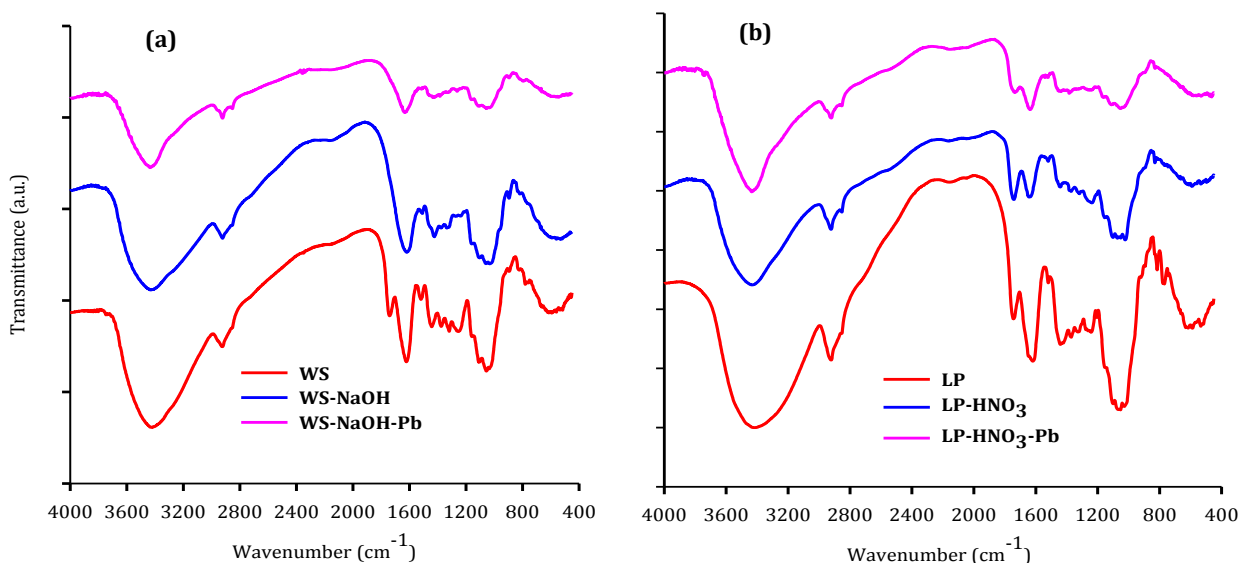


Figure 5. FTIR spectra of (a) WS and (b) LP adsorbent samples

4. Discussion and Conclusion

In this study, the use of adsorbents prepared with acid and base-activated WS and LP were investigated to remove Pb(II) from water samples. While the adsorption efficiency of WS was increased with the base activation, that of LP was increased with the acid activation. For both adsorbents, it was observed that adsorption efficiency was increased when pH was increased from 4 to 6, and it was decreased when pH was increased from 6 to 8. It was determined that adsorption efficiency was decreased when temperature was increased and the adsorption process was occurred as exothermic and spontaneous. It was seen that as Pb(II) concentration was increased, the percentage of its removal was decreased but the adsorption capacity was increased. The maximum adsorption capacity was obtained with a solution including 100 mg L⁻¹ Pb(II) adsorbate solution. For both adsorbents, Pb(II) removal was fast at the first 10 min, then slowed down. While equilibrium data were appropriate with Freundlich model, kinetic model for fitting the experimental data were suitable for a pseudo second-order model.

Acknowledgments

The study was financial supported by Scientific and Technical Research Council of Turkey (TÜBİTAK BİDEP 2209-A, Project application no: 1919B011401094).

References

- [1] Wei, H., Yu, H., Zhang, G., Pan, H., Lv, C., Meng, F. 2018. Revealing the correlations between heavy metals and water quality, with insight into the potential factors and variations through canonical correlation analysis in an upstream tributary. *Ecological Indicators*, 90 (2018) 485-493.
- [2] Waheed, A., Mansha, M., Ullah, N. 2018. Nanomaterials-based electrochemical detection of heavy metals in water: Current status, challenges and future direction. *Trends in Analytical Chemistry*, 105 (2018) 37-51.
- [3] Novais, R.M., Buruberri, L.H., Seabra, M.P., Labrincha, J.A. 2016. novel porous fly-ash containing geopolymer monoliths for lead adsorption from wastewaters. *Journal of Hazardous Materials*, 318(2016), 631-640.
- [4] Schiewer, S., Balaria, A. 2009. Biosorption of Pb²⁺ by original and protonated citrus peels: Equilibrium, kinetics, and mechanism. *Chemical Engineering Journal*, 146(2009), 211-219.
- [5] Yi, L., Wang, W., Wang, A. 2010. Adsorption of lead ions from aqueous solution by using carboxymethyl cellulose-g-poly (acrylic acid)/attapulgitite hydrogel composites. *Desalination*, 259(2010), 258-264.
- [6] Fadzil, F., Ibrahim, S., Hanafiah, M.A.K.M. 2016. Adsorption of lead (II) onto organic acid modified rubber leaf powder: batch and column studies. *Process Safety Environmental Protection*, 100(2016), 1-8.
- [7] Basu, M., Guha, A.K., Ray, L. 2017. Adsorption of lead on cucumber peel. *Journal of Cleaner Production*, 151(2017), 603-615.
- [8] Sema Tofan, Konya Bölgesindeki İçme Sularında Metal Tayini , Yüksek Lisans Tezi , Selçuk Üniversitesi Fen Bilimleri Enstitüsü , KONYA, 2008.
- [9] Hajiaghababaei, L., Badiie, A., Ganjali, M.R., Heydari, S., Khaniani, Y., Ziarani, G.M. 2011. Highly efficient removal and preconcentration of lead and cadmium cations from water and wastewater samples using ethylenediamine functionalized SBA-15. *Desalination*, 266(1-3) (2011), 182-187.
- [10] Momčilović, M., Purenović, M., Bojić, A., Zarubica, A., Randelović, M. 2011. Removal of lead (II) ions from aqueous solutions by adsorption onto pine cone activated carbon. *Desalination*, 276(2011), 53-59.
- [11] Zhao, Z., Zhang, X., Zhou, H., Liu, G., Kong, M., Wang, G. 2017. Microwave-assisted synthesis of magnetic Fe₃O₄-mesoporous magnesium silicate core-shell composites for the removal of heavy metal ions. *Microporous Mesoporous Materials*, 242(2017), 50-58.
- [12] Bhatnagar, A., Sillanpää, M., Krowiak, A.W. 2015. Agricultural waste peels as versatile biomass for water purification—a review. *Chemical Engineering Journal*, 270(2015), 244-271.
- [13] Feng, N., Guo, X., Liang, S. 2009. Adsorption study of copper (II) by chemically modified orange peel. *Journal of Hazardous Materials*, 164(2009), 1286-1292.
- [14] Abdel-Ghani, N.T., El-Chaghaby, G. A. 2014. Biosorption for metal ions removal from aqueous solutions: A review of recent studies. *International Journal of Latest Research in Science and Technology*, 3(2014), 24-42.
- [15] Yong, Z., Zhang, L., Cheng, Z. 2015. Removal of organic pollutants from aqueous solution using agricultural wastes: A review. *Journal of Molecular Liquid*, 212(2015), 739-762.
- [16] Nguyen, T.A.H., Ngo, H.H., Guo, W.S., Zhang, J., Liang, S., Yue, Q.Y., Nguyen, T.V. 2013. Applicability of agricultural waste and by-products for adsorptive removal of heavy metals from wastewater. *Bioresource Technology*, 148(2013), 574-585.

- [17] Nazari, G., Abolghasemi, H., Esmaili, M. 2016. Batch adsorption of cephalosporin antibiotic from aqueous solution by walnut shell-based activated carbon. *Journal of the Taiwan Institute of Chemical Engineers*, 58(2016), 357-365.
- [18] Ngah, W.S.W., Hanafiah, M.A.K.M. 2008. Removal of heavy metal ions from wastewater by chemically modified plant wastes as adsorbents: a review. *Bioresource Technology*, 99(2008), 3935-3948.
- [19] Annadurai, G., Juang, R.S., Lee, D.J. (2003). Adsorption of heavy metals from water using banana and orange peels. *Water Science Technology*, 47 (2003), 185-190.
- [20] Wolfová, R., Pertile, E., Fečko, P. 2013. Removal of lead from aqueous solution by walnut shell. *Journal of Environmental Chemistry and Ecotoxicology*, 5(6)(2013), 159-167.
- [21] Feng, N. C., Guo, X.Y. 2012. Characterization of adsorptive capacity and mechanisms on adsorption of copper, lead and zinc by modified orange peel. *Transactions of Nonferrous Metals Society of China*, 22(5) (2012), 1224-1231.
- [22] Zhong-Liang, S., Li, F., Yao, S.H. 2011. Adsorption behaviors of lead ion onto acetate modified activated carbon fiber. *Desalination and Water Treatment*, 36(2011), 164-170.
- [23] Solmaz, S., Karimi-Jashni, A., Doroodmand, M.M. 2014. Synthesis and characterization of novel single-walled carbon nanotubes-doped walnut shell composite and its adsorption performance for lead in aqueous solution. *Journal of Environmental Chemical Engineering*, 2(2014), 2059-2067.
- [24] Sudha, R., Srinivasan, K., Premkumar, P. 2016. Kinetic, mechanism and equilibrium studies on removal of Pb (II) using Citrus limettoides peel and seed carbon. *Research on Chemical Intermediates*, 42(3) (2016), 1677-1697.
- [25] Bediako, J. K., Reddy, D. H. K., Song, M.H., Wei, W., Lin, S., Yun, Y.S. 2017. Preparation, characterization and lead adsorption study of tripolyphosphate-modified waste lyocell fibers. *Journal of Environmental Chemical Engineering*, 5(2017), 412-421.
- [26] Dubey, A., Shiwani, S. 2012. Adsorption of lead using a new green material obtained from portulaca plant. *International Journal of Environmental Science and Technology*, 9(2012), 15-20.
- [27] Njoku, V.O., Ayuk, A.A., Ejike, E.E., Oguzie, E.E., Duru, C.E., Bello, O.S. 2011. Cocoa pod husk as a low cost biosorbent for the removal of Pb(II) and Cu(II) from aqueous solutions. *Australian Journal of Basic and Applied Sciences*, 5(2011), 101-110.
- [28] Saka, C., Sahin, O., Demir, H., Kahyaoglu, M. 2011. Removal of lead from aqueous solutions using preboiled and formaldehyde treated onion skins as a new adsorbent. *Separation Science and Technology*, 46(2011), 507-517.
- [29] Taha, G.M., Arifien, A.E., El-Nahas, S. 2011. Removal efficiency of potato peels as a new biosorbent material for uptake of Pb(II), Cd(II) and Zn(II) from the aqueous solutions. *The Journal of Solid Waste Technology and Management*, 37(2011), 128-140.
- [30] Lam, Y.F., Lee, L.Y., Chua, S.J., Lim, S.S., Gan, S. 2016. Insights into the equilibrium, kinetic and thermodynamics of nickel removal by environmental friendly lansium domesticum peel biosorbent. *Ecotoxicology and Environmental Safety*, 127(2016), 61-70.
- [31] Agarwal, S., Tyagi, I., Gupta, V. K., Mashhadi, S., Ghasemi, M. 2016. Kinetics and thermodynamics of Malachite Green dye removal from aqueous phase using iron nanoparticles loaded on ash. *Journal of Molecular Liquids*, 223 (2016), 1340-1347.
- [32] Liu, G., Zhang, W., Luo, R. (2018). Synthesis, characterization of amino-modified walnut shell and adsorption for Pb (II) ions from aqueous solution. *Polymer Bulletin*, 2018, 1-16.
- [33] Nag, S., Mondal, A., Roy, D. N., Bar, N., Das, S. K. 2018. Sustainable bioremediation of Cd (II) from aqueous solution using natural waste materials: Kinetics, equilibrium, thermodynamics, toxicity studies and GA-ANN hybrid modelling. *Environmental Technology & Innovation*, 11 (2018), 83-104.
- [34] Sahmoune M.N. 2018. Thermodynamic Properties of Heavy Metals Ions Adsorption by Green Adsorbents. In: Crini G., Lichtfouse E. (eds) *Green Adsorbents for Pollutant Removal*. Environmental Chemistry for a Sustainable World, Vol 18. Springer, Cham.
- [35] Schiewer, S., Patil, S.B. 2008. Pectin-Rich fruit wastes as biosorbents for heavy metal removal: equilibrium and kinetics. *Bioresource Technology*, 99(2008), 1896-1903.
- [36] Febrianto, J., Kosasih, A. N., Sunarso, J., Ju, Y. H., Indraswati, N., Ismadi, S. 2009. Equilibrium and kinetic studies in adsorption of heavy metals using biosorbent: a summary of recent studies. *Journal of Hazardous Materials*, 162(2009), 616-645.
- [37] Ding, D., Zhao, Y., Yang, S., Shi, W., Zhang, Z., Lei, Z., Yang, Y. 2013. Adsorption of cesium from aqueous solution using agricultural residue-walnut shell: equilibrium, kinetic and thermodynamic modeling studies. *Water Research*, 47(2013), 2563-2571.

- [38] Barbosa, J.J.M., López-Velandia, C., Maldonado, A. del P., Giraldo, L., Moreno-Piraján, J.C. 2013. Removal of lead (II) and zinc (II) ions from aqueous solutions by adsorption onto activated carbon synthesized from watermelon shell and walnut shell. *Adsorption*, 19(2013), 675-685.
- [39] El-Kady, A.A., Carleer, R., Yperman, J., D'Haen, J., Abdel Ghafar, H.H. 2016. Kinetic and adsorption study of Pb (II) toward different treated activated carbons derived from olive cake wastes. *Desalination and Water Treatment*, 57(2016), 8561-8574.
- [40] Juan, Y., Qiu, K. 2010. Preparation of activated carbons from walnut shells via vacuum chemical activation and their application for methylene blue removal. *Chemical Engineering Journal*, 165(2010), 209-217.
- [41] Cao, J.S., Lin, J.X., Fang, F., Zhang, M.T., Hu, Z.R. 2014. A new adsorbent by modifying walnut shell for the removal of anionic dye: kinetic and thermodynamic studies. *Bioresource Technology*, 163(2014), 199-205.
- [42] Arslanoglu, H., Altundogan, H.S., Tumen, F. 2008. Preparation of cation exchanger from lemon and sorption of divalent heavy metals. *Bioresource Technology*, 99(2008), 2699-2705.
- [43] Singh, S.A., Shukla, S.R. 2016. Adsorptive removal of cobalt ions on raw and alkali-treated lemon peels. *International Journal of Environmental Science Technology*, 13(2016), 165-178.